Efficiency Improvements For A Synergetic Hydrogen-Methanol Process Chain Using A Seasonal Schedule*

David Wekerle[1], Axel Hackbarth[1] and Klaas Völtzer[1]

***Abstract*— Cross-sector solutions are needed for sustainable industrial production chains. The German project "WEST-KUESTE 100" proposes such a process chain to minimize production costs of green hydrogen and green methanol and make the clinker production more sustainable. Due to the volatility of the renewable energy sources, storage systems for hydrogen, oxygen and carbon-dioxide are necessary. An optimal use of these storages is essential due to the seasonal fluctuations of wind and solar energy production. In this paper, the process chain is modeled, dynamically simulated and controlled by a custom model predictive controller over a time span of 16 years. The custom model predictive controller showed significant improvements in the methanol output with a rising prediction horizon, with a seasonal schedule for the storages.**

I. INTRODUCTION

The goal of this research is to enable efficient and robust operation of a renewable-powered hydrogen-methanol process chain using advanced predictive control strategies. A model predictive controller (MPC) is used with a seasonal storage schedule, aiming to incorporate both short-term weather forecasts and long-term seasonal variability. Additionally, the effects of (move-)blocking on MPC computation time are analyzed. The process chain (Fig. 1) starts with electricity generation from wind farms and photovoltaic (PV) systems for a Proton-Exchange-Membrane (PEM) electrolyzer to produce green hydrogen (H_2). As a byproduct, oxygen (O2), is used to facilitate an oxyfuel process in a cement plant for clinker production, at a distance of 60 kilometers. In the oxyfuel process the combustion is carried out with O_2 instead of air, yielding a high-purity carbon dioxide (CO_2) exhaust gas stream. This CO_2 is captured and used in addition with the produced H_2 to synthesize methanol. The methanol will be used as fuel for ships. Conventional above-ground tanks serve as intermediate storage for liquid O_2 and CO_2, while an existing cavern storage facility is used for the gaseous H_2. Any surplus H_2 is channeled into the natural gas grid via a pipeline. The WESTKUESTE100 process chain is described in detail in an earlier publication [1].

A multitude of publications are available for the PEM-electrolysis [2], [3]. The methanol synthesis has been analysed technically and economically by Teles et al. [4]. Cavern storage systems for H_2 and their mathematical models were assessed by Li et al. in [5] and Jeannin et al. in [6]. Different forms of green hydrogen methanol process chains have been examined technically, economically and ecologically by Ciancio et al. and Sollai et al. [7], [8]. The sizes of the individual components of the process chain were determined in an overarching optimization considering the economic and technical relations as well as the uncertainties of the RES [9]. Various strategies exist for managing energy in microgrids. Thaler et al. proposed an MPC approach for systems with seasonal hydrogen storage, combining data-driven forecasts with rule-based heuristics [10]. Others have explored hierarchical MPC for wind-hydrogen systems [11] and robust scheduling under hydrogen constraints [12]. In contrast, this work targets a renewable-powered hydrogen-methanol chain, using MPC with short-term forecasts and a seasonal storage schedule to prepare for dark doldrums by storing more H_2 and CO_2 ahead of spring and autumn. Model predictive control (MPC) is a control strategy widely used in different process chains. Its application spans across various industries, including chemical, petrochemical, food processing, and pharmaceuticals [13]. Despite the computational challenges, the ability of MPC to tackle multi-variable control problems and the possibility to introduce constraints make it particularly suitable for optimizing process chains.

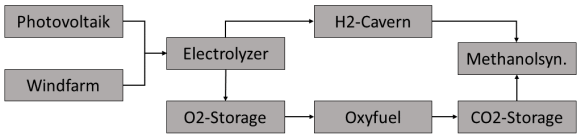

Fig. 1: Westküste100 process chain

II. METHODS

This chapter presents the methods required to investigate the MPC. The model is based on an earlier publication with a special focus placed on the various energy storages, their input- and output- limits and most importantly the linearity of the model to facilitate a fast simulation time [1]. The sample time of the different model components is a global variable. To allow for fast simulation times it was set to 1 hour, enabling a continuous simulation of 15 years.

A. Wind and PV park

The electrical power output of the wind and PV park is calculated for a given wind speed or global radiation. The *turbulence optimized park model* was used by the project partner Oersted to calculate the power output of a wind

*This work was supported by the German Federal Ministry for Economic Affairs and Climate Action

[1]David Wekerle, Axel Hackbarth and Klaas Völtzer are with the Institute for the Transformation of the Energysystem, Fachhochschule Westküste, 25746, Heide, Germany wekerle@fh-westkueste.de - a.hackbarth@fh-westkueste.de - voeltzer@fh-westkueste.de

farm at an offshore location off the German North Sea coast [14]. This model focuses on the wake losses of the wind park. For the PV park, the PVGIS/SAHRA data set from the European commission at a location near Heide, Schleswig-Holstein was used to access global radiation data [15]. Both datasets range from the 1st of January 2005 to the 31st of December 2020. The resulting power was calculated on the basis of 1 MW to reach a peak output of 2.8 GW and 0.3 GW respectively. An additional emphasis was placed on the examination of the time series with regard to dark doldrums. The term 'dark doldrums' describes periods with minimal wind and solar activity, during which renewable energy generation significantly drops, posing challenges for grid stability and energy supply.

B. Electrolysis

The electrolyzer was simplified by means of characteristic curves for efficiency and hydrogen production. The complex electrolysis process is simplified to improve calculation speed. Changes in electrical load were neglected, due to the sample time of one hour greatly exceeding the response time of PEM-electrolysis of less than a minute for idle to nominal power and less than 5 minutes to reach operating pressure. Neglecting the operating states of the electrolyzer does not add any significant error, as the sample time is set to an hour and the ramp up and down times of the PEM electrolyzer are shorter than 20 minutes [16]. Furthermore, the individual modules are each only 0.21% of the nominal power, making the error of load changes small. The efficiency and production data were derived from a 6 MW electrolysis system [17]. The efficiency curve for the 2.8 GW scale was created under the assumption that the electrolyzer modules are so controlled that as many modules are active as necessary to utilize the optimum efficiency. The resulting efficiency and production data can be seen in Figure 2. The model does not include any degradation for the electrolyzer as it is already included on the module level.

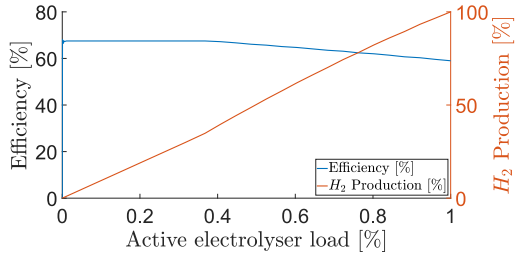

Fig. 2: Efficiency and hydrogen output of the scaled GW electrolyzer

C. Oxyfuel Process

Burning clinker in an oxyfuel process is more efficient than using air for combustion as less gas needs to be circulated. Furthermore, the exhaust CO_2 is much purer (99.97%), which allows the exhaust gas to be used for further processing without the need for gas purification. The cement produced from the clinker is used for construction projects throughout Schleswig-Holstein, Germany. Production targets are the most important factor. Therefore, a 24/7 use of the oxyfuel process is of highest priority, for which a sufficient supply of O_2 is necessary.

D. Methanol Synthesis

Methanol synthesis is a key process in the chemical industry, carried out mainly through catalytic hydrogenation of carbon monoxide (CO) and CO_2 as in equations 1 and 2.

$$\mathrm{CO} + 2\,\mathrm{H_2} \longrightarrow \mathrm{CH_3OH} \tag{1}$$

$$\mathrm{CO_2} + 3\,\mathrm{H_2} \longrightarrow \mathrm{CH_3OH} + \mathrm{H_2O} \tag{2}$$

The power can be changed quickly compared to the sample time, so that static operating points and their linear interpolation can be used, which are taken from an Aspen simulation by the project partner *Thyssen Krupp*.

E. Gas Storages

The storage systems make it possible to compensate for fluctuations in RES. For the storage model, the surpluses of H_2, O_2 and CO_2 are integrated and percentage losses are calculated and deduced for each time step. Storage limitations are specified by tank types and tank volumes. The parameters for the storage systems are listed in Table I.

Product	Min. Level	Max. Level	Storage Losses	Storing Costs
Unit	[t]	[t]	[%/h]	[kWh/t]
O_2	0	10000	0.01208 [18]	98 (Assumption)
CO_2	0	130000	0.00583 [18]	88 [19]
H_2	800	1500	0.00417 [20]	1700 [21]

TABLE I: Main parameters of the storage blocks

1) CO_2 and O_2 Storage Tanks: O_2 and CO_2 are stored in liquid form. As a result, the tanks can be completely emptied. Boil-off losses in storage tanks for CO_2 and O_2 are caused by the transfer of heat from the surrounding environment to the cryogenic liquid within the tanks. The liquid evaporates because of this heat transfer, increasing the pressure inside the tank. The estimated daily losses for O_2 are 0.29% and 0.14% for carbon dioxide [18].

2) H_2 - Cavern Storage: In contrast to the other products, H_2 is stored in gaseous form in a cavern. The cavern storage for H_2 was evaluated by the project partner *Raffinerie Heide*. The cavern pressure must be maintained above a certain threshold (cushion gas) to ensure structural integrity is not compromised. The maximum storage level was determined from the cavern volume and the gas properties of H_2 [22]. Another limitation is the caverns pressure play. The pressure at every timestep must be within $\pm$ 10 bar compared to the pressure 24 hours ago, it may exceed this limit in between the 24 hour period. Therefore, the pressure play limits and the absolute limits are compared and the stricter limit is chosen. Since H_2 readily diffuses through other materials, diffusion losses occur in salt cavern storages. The losses are estimated to be 0.1% per day [20]. Using a cavern to store H_2 requires cleaning the H_2 when it leaves the cavern. The energy consumption of cleaning and compressing is approximately $1700\,\mathrm{kWh/t_{H_2}}$ [21].

F. Linear MPC with Move-Blocking

By utilizing a model of the system to predict future states, MPC allows to apply optimized control inputs to minimize deviations from a desired set point over a prediction horizon. This method is especially effective in process chains with complex dynamics resulting from interactions between different processes. Figure 3 shows a generalized architecture of a MPC. The MPC receives the current state of the plant as well as a prediction for the RES input, predicts future plant outputs using an internal model and minimizes a cost function over a finite, receding horizon by calculating an optimal sequence of control actions. These actions are determined by solving a constrained optimization problem. Only the first element of the resulting array of control actions is applied to the plant. At each subsequent time step, the procedure is repeated, using the latest available information.

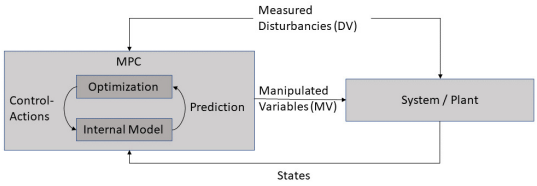

Fig. 3: General MPC structure

A MPC was developed to control the overall system. The MPC controls the storage levels according to a previously determined seasonal schedule (II-G). Using a seasonal schedule helps in preparing for dark doldrum events by filling up the storages before they most frequently occur. The RES are implemented as disturbance variables (DV). For solving the optimization problem, the MPC-Block in Simulink is used [23], [24]. Internally, it uses the KWIK algorithm to solve the general optimization problem.

Equation 3 shows the constraints used for the MPC controlling the process chain, with x(1) being the H_2-storage, x(2) the CO_2-storage and u(1) the operating point for the methanol synthesis.

$$\begin{array}{rcll} \text{x(1)} & \leq & & \text{Maximum Level } H_2 \\ \text{- x(1)} & \leq & \text{-} & \text{Minimum Level } H_2 \\ \text{x(2)} & \leq & & \text{Maximum Level } CO_2 \\ \text{- x(2)} & \leq & \text{-} & \text{Minimum Level } CO_2 \\ \text{u(1)} & \leq & & 100\ \% \\ \text{- u(1)} & \leq & \text{-} & 10\ \% \end{array} \tag{3}$$

(Move) Blocking enables higher computing speeds by increasing the sampling time of the internal model for more distant time steps of the prediction horizon, thus combining several of these distant future time points. This extends the prediction horizon given by the computing resources [25], but it also deprives the MPC of flexibility for the later time steps, as the manipulated variables can then only be adjusted once for the entire block [26]. The move-blocking was implemented dependant on the prediction horizon and two variables $blocking\_start$ and $blocking\_factor$. $blocking\_start$ defining the timespan that should be considered hourly and $blocking\_factor$ the amount of hours that should be considered as one block. Then the amount of blocks results to $n_{Blocks} = (N - blocking\_start)/blocking\_factor$. With a prediction horizon $N = 160$, $blocking\_start = 8$ and $blocking\_factor = 8$ this means $n_{Blocks} = 19$. Allowing to reduce the hessian matrix dimensions from 160 x 160 to 27 x 27 and greatly reduce the compute time. Equation 4 shows the cost function for the MPC with reference tracking, with x as the states, ref as the reference values and w being the weights applied to the different parts of the function.

$$\begin{aligned} cost\_function_{\ ref} = &+ [x(1) - ref(1)] \cdot w_{H_2} \\ &+ [x(2) - ref(2)] \cdot w_{CO_2} \\ &+ m^2_{CO_2\ blowoff} \cdot w_{blowoff} \end{aligned} \tag{4}$$

G. Seasonal Schedule

This seasonal schedule was created in an extra simulation with a sample time of 1 hour and a prediction horizon of 2 months. The $blocking\_start$ and the $blocking\_factor$ parameters were set to 12 hours. Resulting in a prediction horizon of 1452 hours in 12 one hour blocks and 120 12 hour blocks totalling to hessian matrix dimensions of 132 x 132. Each year was considered individually and the resulting curves were averaged. In order to create the seasonal schedule a monetary cost function according to equation 5 was used. m_{H_2} being the surplus of H_2, $m_{methanol}$ the amount of methanol, $E_{electricity}$ the surplus of electricity and $m_{CO_2\ blwoff}$ the CO_2 being blown-off due to full storage. This seasonal schedule enables trajectory tracking for the storages.

$$\begin{aligned} cost\_function_{\ monetary} = &+ m_{H_2} \cdot p_{H_2} \\ &+ m_{methanol} \cdot p_{methanol} \\ &+ E_{electricity} \cdot p_{electricity} \\ &- m_{CO_2\ blowoff} \cdot p_{CO_2\ blowoff} \end{aligned} \tag{5}$$

The future prices for hydrogen, methanol, electricity and the costs for blowing off CO_2 are a big uncertainty. Therefore, pessimistic prices as in Table II are assumed for the cost function.

Symbol	Product	Price	Unit
p_{H_2}	Hydrogen	1500	€/t
$p_{methanol}$	Methanol	2000	€/t
$p_{electricity}$	Electricity	100	€/MWh
$p_{CO_2\ blowoff}$	Carbon-dioxide	200	€/t

TABLE II: Assumptions for product prices

H. CapEx - OpEx

In order to compare different control strategies, the methanol production costs are a valuable indicator. Therefore, Table III shows the Capital Expenditures (CapEx) and Operational Expenditures (OpEx) used in order to calculate the costs of the system.

To get the total cost of ownership (TCO) the CapEx are summed and then multiplied with the interest rate to the power of operating years. The OpEx of the subsystems is

Name	CapEx		OpEx		Source
	Cost	Unit	Cost	Unit	
Wind park	$2.5 \cdot 10^6$	€/MW nom. Cap.	0.02	share of CapEx	[27]
PV park	$0.25 \cdot 10^6$	€/MW nom. Cap.	0.02	share of CapEx	[27]
Elektrolyseur	$1.2 \cdot 10^6$	€/MW nom. Cap.	0.03	share of CapEx	[28]
Methanol syn.	$8 \cdot 10^6$	€/(t/h) nom. Cap.	0.05	share of CapEx	[29]
H_2 cavern	$0.3 \cdot 10^6$	€/t nom. Cap.	0.03	share of CapEx	[30], [31]
O_2 storage	$0.001889 \cdot 10^6$	€/t nom. Cap.	0.02	share of CapEx	[18]
CO_2 storage	$0.001889 \cdot 10^6$	€/t nom. Cap.	0.1	share of CapEx	[19]

TABLE III: Assumptions for CapEx & OpEx of the systems

calculated as a share of the CapEx. The individual OpEx are then totaled and multiplied by the number of years under consideration as in equation 6. The operating years were set to 16 and an interestrate of 5% was assumed.

$$TCO = CapEx \cdot (1+Interestr.)^{Years} + OpEx \cdot Years \quad (6)$$

Based on this, the minimum required methanol price can be calculated, according to equation 7.

$$p_{methanol} = \frac{TCO + Penalties_{CO_2} - Revenue_{H_2 \& Elec.}}{m_{methanol}} \quad (7)$$

III. Results and Discussion

The dark doldrum events are analyzed first. Subsequently, the simulation results for constant weights of reference deviations of the storages in the MPC are shown. Then the prediction horizons are varied and move-blocking is tested. Finally, the seasonal schedule and the economics of the process chain are analyzed.

A. Dark Doldrums

To identify dark doldrums, a $threshold$ parameter was implemented for the relative power input to prevent artificial separation into multiple shorter events. Figure 4 shows the duration of the 10 longest events at thresholds from 10% to 50% with the colors indicating the length of the dark doldrums. An additional parameter $threshold\_hours$ was

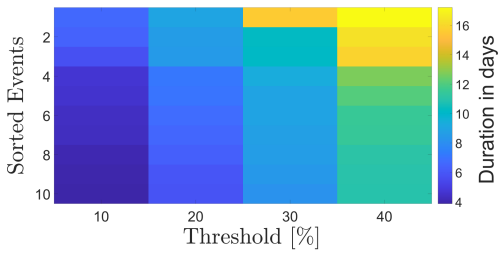

Fig. 4: Durations of the longest dark doldrum Events dependent on $threshold$ parameter

added to avoid separating the events in case of short-term medium to high power. If the time period in between identified events is shorter than the $treshold\_hours$, the two events are combined into one. Figure 5 shows the duration of the 10 longest events depending on the $threshold\_hours$

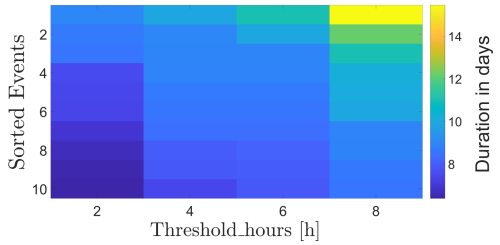

Fig. 5: Durations of the longest dark doldrum Events dependent on $threshold\_hours$ parameter

parameter with $threshold = 30\%$. The parameters were fixed to $threshold = 25$ % and $threshold\_hours = 6$ hours, resulting in maximum durations of up to 11 days.

B. Constant Weights

Figure 6 shows the resulting storage levels for H_2 and CO_2 for a simulation period of one year with equal weights. As can be seen, the CO_2-storage stays on the reference for the entire simulation, whereas the H_2-storage does not follow the target. That is due to the the limitations from the pressure play and the more direct influence of the RES compared to the CO_2-storage, sitting behind the intermediate O_2 storage and the oxyfuel process.

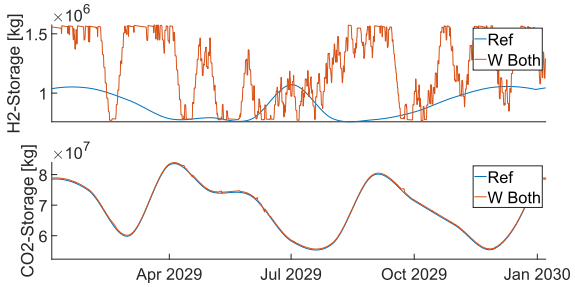

Fig. 6: Resulting storage levels with MPC using the seasonal schedule

When only the reference deviaton of the CO_2 storage is weighted and the CO_2 blow-off is weighted quadratically, the system does not blow off any CO_2. Due to the fluctuations of the renewable energy and the limitations on the pressure play, the H_2 storage cannot follow the reference. This means that during dark doldrum events, the H_2 storage runs empty in 24-48 hours, as the storage is not completely

filled. The time depends on the level and the intensity of the dark doldrum.

C. Prediction Horizons

To measure the improvements resulting from an increasing prediction horizon, several criteria are examined: the compute time, the control quality in the form of normalized root mean square error (NRMSE) and the revenue of methanol and hydrogen, which is sold as the cavern storage is full. Figure 7 shows the results for a prediction horizon from 10 to 160 hours in 10 hour steps for a simulation period of one year each. The compute time is given in minutes and increases quadratically on a regular PC. The NRMSE falls by 1 % and the methanol output rises by about 0.2 % per simulation year. H_2 has to be sold directly less frequently and CO_2 has to be blown off less frequently. It should be considered though, that the forecast for the RES is perfect over the whole prediction horizon in this simulation. While in reality, short-term forecast errors are typically small, rare events such as dark doldrums can still challenge MPC performance and system reliability.

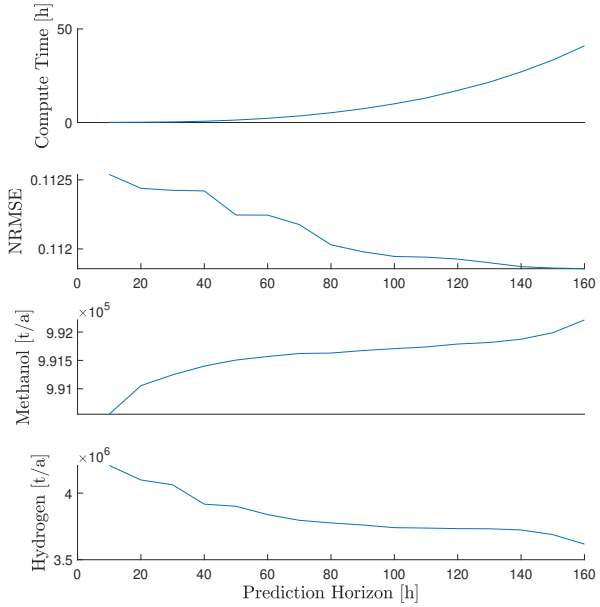

Fig. 7: Compute time, NRMSE, methanol and sold hydrogen for 1 year over the prediction horizon from 10 h to 160 h

The MPC with the move blocking feature was tested in direct comparison to the MPC without. Figure 8 compares the compute time and control quality of the two variants of the MPC over a simulation period of one year. The *blocking_start* and *blocking_factor* parameters were both set to 8 hours. As the control quality stays the same for both variants, the compute times for the blocking MPC are lower. This effect gets stronger with increasing prediction horizons.

D. Seasonal Schedule

The MPC with a seasonal schedule is compared to a MPC with the cost function described in Equation 5. The process chain doesn't emit any CO_2 with either MPC variants over

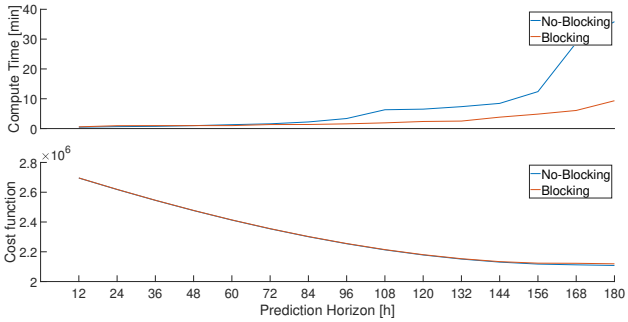

Fig. 8: Compute time and NRMSE for 1 year over the prediction horizon from 12 to 192 h for regular MPC and move-blocked MPC

the simulation time of 16 years. Figure 9 shows the H_2 and CO_2 storages for one sample year from the 16 year simulation period. As can be seen the MPC with the cost function stores CO_2 more constant as the MPC with the seasonal schedule. The latter can produce more methanol, while the MPC with the cost function sells more hydrogen directly, when the cavern storage is full. The resulting average price for methanol with the cost function MPC is 1860 € and 1810 € with the seasonal schedule. Therefore, the seasonal schedule improves the price by 2.5 %. The full-load-hours of the electrolyzer using the seasonal schedule is approx. 4500h.

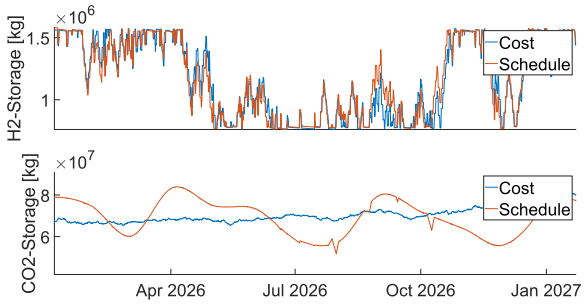

Fig. 9: Comparison between MPC with seasonal schedule and cost function

E. Economics

To analyze the economics of the system, equations 6 and 7 are used. The prediction horizon was set to 160 with move-blocking enabled as in III-C. With an interest rate of 5% the resulting methanol price reaches 1810 € while using the seasonal schedule. Assuming a market price of roughly 2000 €/t for green methanol, the break-even point is reached after approximately 8 years. These results heavily depend on the uncertain prices of electricity, H_2 and methanol, that are being assumed for calculation.

IV. Conclusions and Outlook

This paper shows that using a MPC with a predefined seasonal schedule can increase the methanol output of the process chain and therefore reduce the methanol price. As a

result the performance of the MPC is not dependent on long-term weather forecasts. This is a great advantage due to the increasing uncertainty of the weather forecast as the prediction horizon rises. The usage of move-blocking in the MPC can decrease compute time significantly, allowing longer prediction horizons and simulation times being realized on standard PC. The influence of an additional battery storage between the RES and the electrolyzer should be analyzed in the context of full-load-hours and peak shaving. Furthermore, the effects of additional storage capacity on the process chain during periods of low renewable generation (dark doldrums) will be explored. Future work will also address the required battery capacity, the potential for downsizing the electrolyzer, and the optimal trade-off between short-term weather forecasts and long-term seasonal scheduling.

ACKNOWLEDGMENT

The Westküste100 project received funding approval in the area of sector coupling and hydrogen technologies as part of the "Real-world laboratories of the energy transition". The real-world laboratories are funded by the Federal Ministry for Economic Affairs and Climate Action as part of the 7th Energy Research Program and aim to test innovative technologies on an industrial scale under real conditions.

Supported by:

on the basis of a decision
by the German Bundestag

REFERENCES

[1] D. Wekerle and K. Völtzer, "Vorstellung einer ökonomischen fahrweise für eine wasserstoff-methanol prozesskette – westküste100," *Sammelband: Wasserstoff-Forschung SH KOMPAKT*, 2024.

[2] F. Barbir, "PEM electrolysis for production of hydrogen from renewable energy sources," *Solar Energy*, vol. 78, no. 5, pp. 661–669, 2005. Solar Hydrogen.

[3] S. Shiva Kumar and V. Himabindu, "Hydrogen production by pem water electrolysis – a review," *Materials Science for Energy Technologies*, vol. 2, no. 3, pp. 442–454, 2019.

[4] M. Teles, M. Bram, H. R. Shabani, S. Shoja Majidabad, J. Liniger, and X. Cui, "Optimization and 3e analysis on variable operational conditions of a large, medium and small size green methanol plant," *Energy Conversion and Management*, vol. 300, p. 117870, 01 2024.

[5] J. Li, X. Shi, C. Yang, Y. Li, T. Wang, and H. Ma, "Mathematical model of salt cavern leaching for gas storage in high-insoluble salt formations," *Scientific Reports*, vol. 8, 01 2018.

[6] L. Jeannin, A. Myagkiy, and A. Vuddamalay, "Modelling the operation of gas storage in salt caverns: numerical approaches and applications," *Science and Technology for Energy Transition*, vol. 77, p. 6, 05 2022.

[7] A. Ciancio, A. Mojtahed, and A. Sgaramella, "Decarbonization of methanol production - techno-economic analysis of power-to-fuel process in a hydrogen valley," *Journal of Physics: Conference Series*, vol. 2648, p. 012066, 12 2023.

[8] S. Sollai, A. Porcu, V. Tola, F. Ferrara, and A. Pettinau, "Renewable methanol production from green hydrogen and captured co2: A techno-economic assessment," *Journal of CO2 Utilization*, vol. 68, p. 102345, 2023.

[9] T. Cors, M. Fliedner, K. Völtzer, and D. Hustadt, "Green hydrogen value chain design under uncertainty," pp. 95–151, 2024.

[10] B. Thaler, S. Posch, A. Wimmer, and G. Pirker, "Hybrid model predictive control of renewable microgrids and seasonal hydrogen storage," *International Journal of Hydrogen Energy*, vol. 48, no. 97, pp. 38125–38142, 2023.

[11] M. Bakr Abdelghany, V. Mariani, D. Liuzza, and L. Glielmo, "Hierarchical model predictive control for islanded and grid-connected microgrids with wind generation and hydrogen energy storage systems," *International Journal of Hydrogen Energy*, 08 2023.

[12] C. Huang, Y. Zong, S. You, C. Træholt, Y. Zheng, J. Wang, Z. Zheng, and X. Xiao, "Economic and resilient operation of hydrogen-based microgrids: An improved mpc-based optimal scheduling scheme considering security constraints of hydrogen facilities," *Applied Energy*, vol. 335, p. 120762, 04 2023.

[13] C. B. E. F. Camacho, "Model predictive control," *Advanced Textbooks in Control and Signal Processing*, pp. XXII, 405, 2004.

[14] N. G. Nygaard, S. T. Steen, L. Poulsen, and J. G. Pedersen, "Modelling cluster wakes and wind farm blockage," *Journal of Physics: Conference Series*, vol. 1618, p. 062072, sep 2020.

[15] T. Huld, R. Müller, and A. Gambardella, "A new solar radiation database for estimating pv performance in europe and africa," *Solar Energy*, vol. 86, no. 6, pp. 1803–1815, 2012.

[16] International Renewable Energy Agency (IRENA), "Green hydrogen cost reduction: Scaling up electrolysers to meet the 1.5°c climate goal," 2020.

[17] M. Kopp, *Strommarktseitige Optimierung des Betriebs einer PEM-Elektrolyseanlage*. kassel university press GmbH, 2018.

[18] Linde AG - Engineering Division, "Leading international tank standard," 2021. https://assets.linde.com/-/media/global/engineering/engineering/home/products-and-services/plant-components/cryogenic-tanks/lits-technical-data.pdf, Accessed 12.01.2024.

[19] Element Energy, "Shipping co2 - uk cost estimation study," Nov. 2018.

[20] A. Amid, D. Mignard, and M. Wilkinson, "Seasonal storage of hydrogen in a depleted natural gas reservoir," *International Journal of Hydrogen Energy*, vol. 41, no. 12, pp. 5549–5558, 2016.

[21] M. Khan, C. Young, C. MacKinnon, and D. Layzell, "The techno-economics of hydrogen compression.," *Transition Accelerator Technical Briefs Vol. 1*, vol. Issue 1, pp. 1–36, 2021.

[22] Eric W. Lemmon, Ian H. Bell, Marcia L. Huber, and Mark O. McLinden, *Thermophysical Properties of Fluid Systems*. Gaithersburg MD, 20899: National Institute of Standards and Technology, 2023. DOI: https://doi.org/10.18434/T4D303, Accessed 15.01.2024.

[23] The MathWorks Inc., "Simulink version: 10.7 (r2023a)." https://www.mathworks.com, 2023 (accessed 20.01.2024).

[24] The MathWorks Inc., "Model predictive control toolbox version: 8.1 (r2023a)." https://www.mathworks.com, 2022 (accessed 20.01.2024).

[25] Schwenzer, M., Ay, M., Bergs, T. et al., "Review on model predictive control: an engineering perspective," *Int J Adv Manuf Technol 117*, p. 1327–1349, 2021.

[26] R. C. Shekhar and C. Manzie, "Optimal move blocking strategies for model predictive control," *Automatica*, vol. 61, pp. 27–34, 2015.

[27] L. Sens, U. Neuling, and M. Kaltschmitt, "Capital expenditure and levelized cost of electricity of photovoltaic plants and wind turbines – development by 2050," *Renewable Energy*, vol. 185, pp. 525–537, 2022.

[28] A. H. Reksten, M. S. Thomassen, S. Møller-Holst, and K. Sundseth, "Projecting the future cost of pem and alkaline water electrolysers; a capex model including electrolyser plant size and technology development," *International Journal of Hydrogen Energy*, vol. 47, no. 90, pp. 38106–38113, 2022.

[29] K. Atsonios, K. D. Panopoulos, and E. Kakaras, "Investigation of technical and economic aspects for methanol production through co2 hydrogenation," *International Journal of Hydrogen Energy*, vol. 41, no. 4, pp. 2202–2214, 2016.

[30] D. Papadias and R. Ahluwalia, "Bulk storage of hydrogen," *International Journal of Hydrogen Energy*, vol. 46, no. 70, pp. 34527–34541, 2021.

[31] S. Cloete, O. Ruhnau, and L. Hirth, "On capital utilization in the hydrogen economy: The quest to minimize idle capacity in renewables-rich energy systems," *International Journal of Hydrogen Energy*, vol. 46, no. 1, pp. 169–188, 2021.